

액정 배향용 하이브리드 AlTiSrO/rGO 박막 제조 및 특성 평가

오병윤*

Fabrication and characterization of hybrid AlTiSrO/rGO thin films for liquid crystal orientation

Byeong-Yun Oh*

요약 환원된 산화 그래핀(rGO)을 알루미늄, 티타늄, 스트론튬이 혼합된 졸-겔 용액에 혼합하여 브러시 코팅법을 이용하여 액정배향용 하이브리드 박막을 제조하였다. 160, 260, 및 360°C에서 어닐링한 후 산화 반응의 차이를 관찰하였다. 박막 제조 과정에서 생성된 졸-겔 용액은 브러시 모의 전단 응력에 의해 수축력을 발생시켜 미세홈 구조를 형성하였다. 이러한 구조는 주사 전자 현미경 분석을 통해 확인되었으며, rGO의 존재가 명확하게 보였다. 어닐링 온도가 증가함에 따라서 박막 표면의 산화 및 환원 반응이 더욱 활성화되어 표면 혼합물의 강도가 증가하였다. 또한 혼합물의 강도를 증가시킴으로써 전기광학적 특성이 안정화되고 개선되었다. 더불어 전압-정전용량 값도 크게 향상되었다. 최종적으로 투과율 측정 결과 액정디스플레이의 액정 배향막으로 적용하기에 적합한 것으로 나타났다.

Abstract A hybrid thin film was prepared by doping reduced graphene oxide (rGO) into a sol-gel solution mixed with aluminum, titanium, and strontium using a brush coating method. The annealing temperature was carried out at 160, 260, and 360°C, and the difference in oxidation reaction was observed. The sol-gel solution created during the membrane manufacturing process generates a contractile force due to the shear stress of the brush bristles, forming a microgroove structure. This structure was confirmed through scanning electron microscopy analysis, and the presence of rGO was clearly revealed. As the annealing temperature increases, the oxidation and reduction reactions on the thin film surface become more active, so the intensity of the surface mixture increases. Moreover, the electro-optical properties were stabilized and improved by increasing the intensity of the mixtures. Likewise, the voltage-capacitance values are also significantly improved. Lastly, the transmittance measurement showed that it was suitable for liquid crystal display application.

Key Words : AlTiSrO/rGO thin film, Brush coating, Graphene oxide, Liquid crystal orientation, Sol-gel method

1. INTRODUCTION

Due to the recent rapid development of electronic devices and increasing demand for advanced display technology, extensive research has been conducted in various nanotechnology fields such as nanosensors[1],

nanostructures[2], nanofilters[3], nanogels[4], and nanomembranes[5]. To produce these films, the study of surface morphology has emerged as an important strategy in modern engineering. Moreover, advances in modern nanotechnology have had a significant impact on the improvement of integrated circuits and

*Corresponding Author : Research and Development Department, Cheomdanlab Inc. (ohnleeu@nate.com)

Received June 01, 2024

Revised June 11, 2024

Accepted June 17, 2024

the fabrication of high-quality nanostructures on desired substrates. In particular, the surface of micro-nanogroove structures significantly improves the performance of functional devices in biological, optical, mechanical, and electrical responses compared to flat surfaces. In electro-optical (EO) engineering, manipulating surface strain can control device properties by creating surface anisotropy and modulating surface energy. Nanostructures exhibiting wave and quasi-periodic properties play an important role in improving the optical properties of solar cells and optical applications such as organic light-emitting diodes and displays. Additionally, in the display field, thin film transistor structures are used for each pixel in the displays of various electronic devices such as televisions, cameras, automobile displays, smartphones, and monitors. Manufacturing industries typically use methods such as friction, evaporation, electron beam lithography, and UV lithography to produce these films. It is worth noting that polyimide (PI) films produced through friction can generate chips and scratches on the film surface, potentially damaging electronic devices[6, 7].

Conventional rubbing treatment remains an effective means of aligning liquid crystal (LC) molecules in LC display (LCD) manufacturing. Current rubbing methods, known for their simplicity, reliability, and cost-effectiveness, are widely used in the LCD industry[8-11]. At the same time, we propose a brush coating method that controls the directional coating of thin films through blade coating, bar coating, and brush coating. This method minimizes damage to the thin film while maintaining the advantage of friction. Brush coating allows high

throughput by applying the solution to brush bristles, enabling anisotropic surface control, directional control through shear stress, simultaneous film deposition, and fast and efficient film alignment.

In modern electronics, the EO properties depend on the selected thin film fabrication method and material. Transparent conductive oxides (TCOs) are commonly used in various applications and offer high-performance electrical properties such as transparency and conductivity[12]. A typical example is the application of an indium tin oxide (ITO) film, which is known to have low electrical resistance and high transparency to visible light[13]. Despite these impressive properties, ITO materials suffer from toxicity, high cost, and lack of flexibility. Accordingly, studies on inorganic materials with good EO properties are being conducted.

Recently, research on forming a thin film by introducing and mixing simple inorganic materials and carbon-based materials such as fullerene[14], carbon nanotubes[15], and graphene[16-18] has been conducted in various fields. In particular, graphene has emerged as an excellent material with excellent electrical, thermal, and mechanical properties, characterized by the fact that the sp^2 -bonded carbon atom is composed of a single atomic layer in a two-dimensional structure. Due to its high carrier mobility, the unique bandgap structure[19-21] is ideal for future optoelectronic device applications. However, it is difficult to obtain large-area thin films for applications such as high-speed nanotransistors and transparent conductive films. In this case, reduced graphene oxide (rGO) is used as an alternative to graphene

nanosheets. Unlike graphene sheets, rGO integrates sp^2 and sp^3 hybrid carbon. This is because most sp^3 hybrid carbon atoms form covalent bonds with oxygen, creating unique atomic and electronic structures. The functionality is further improved by the introduction of epoxy and hydroxyl groups. In particular, rGO exhibits a bandgap of about 1.7 eV at room temperature, making it very suitable as a semiconductor material. Recent reports have highlighted thin films using rGO as an electron-soluble material for organic solar cells due to their unique structure, electrical properties, and electrochemical properties, attracting significant research interest.

In this study, rGO-doped AlTiSrO (AlTiSrO/rGO) thin films for use as transparent conductive films were fabricated using the sol-gel method. The chemical composition and surface properties of the brush-coated AlTiSrO/rGO hybrid thin films were examined using energy dispersive spectroscopy (EDS, JEM-F200, JEOL). The investigation was performed using UV-Vis Spectrophotometers (V-650, JASCO Corp.). Finally, response time-transmittance analysis and voltage-transmittance analysis were used to analyze the capacitance, voltage characteristics, and EO characteristics of the thin film.

2. EXPERIMENTS

2.1 Preparation of hybrid solutions for thin film manufacturing

The AlTiSrO solution was prepared by mixing 0.1 mol each of aluminum nitrate dihydrate ($Al(NO_3)_3 \cdot 9H_2O$), titanium(IV) oxide

(TiO_2), and strontium nitrate ($Sr(NO_3)_2$). Then, 2-methoxyethanol (2ME) was added to the solution and the mixture was heated and stirred at $70^\circ C$ and 320 rpm for 1 hr. The mixture was then aged for 1 day to obtain a stable solution. For display properties, graphene oxide ($C_xO_yH_z$, dispersion in H_2O , Sigma-Aldrich Korea Co., Ltd.) was dissolved in 2ME at 5 wt%. The AlTiSrO solution was then doped with 20 wt% rGO to prepare the hybrid solution as shown in Figure 1(a). Afterwards, it was annealed at temperatures of 160, 260 and $360^\circ C$. ITO glass (Samsung Corning 1737, $32 \times 22 \times 1.1 \text{ mm}^3$, sheet resistance 10 sq^{-1}) was used as a thin film manufacturing substrate. To treat the surface of the substrate, ultrasonic cleaning was performed using acetone and isopropyl alcohol for 10 minutes, followed by washing with deionized water and drying with N_2 gas.

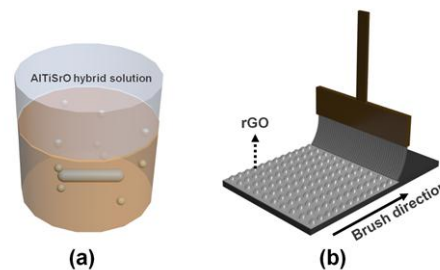


Fig. 1. (a) Manufacturing AlTiSrO/rGO hybrid solution through a sol-gel process, (b) the hybrid thin film is manufactured by brush coating

그림 1. (a) 졸-겔 공정을 통해 AlTiSrO/rGO 하이브리드 용액 제조, (b) 브러시 코팅을 통해 하이브리드 박막 제조

2.2 AlTiSrO/rGO via brush coated thin film manufacturing

For a consistent experiment, the brush was immersed in a AlTiSrO/rGO solution, which

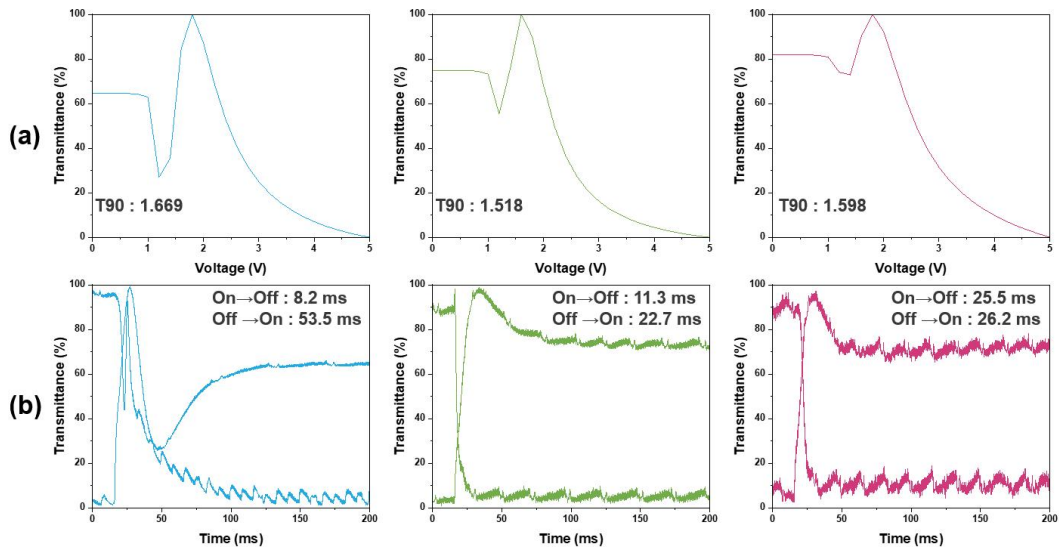


Fig. 2. (a) VT and (b) RT curves based on the measurement of electro-optical properties of 160, 260, and 360°C

그림 2. 160, 260, 및 360°C의 전기광학 특성 측정을 기반으로 한 (a) VT 및 (b) RT 곡선

was then applied to the brush hair and affixed to the brush pin. We used a flat brush made of nylon bristles (900A, ALPHA CO., Ltd.) for brush coating. The substrate was placed on the stage and secured under vacuum. The stage moved at a constant speed resembling a conveyor belt, with the x-axis speed controlled by the controller.

2.3 Fabrication of LC Cells and Evaluation of Characteristics

TN cell was fabricated to measure the electrical and orientation characteristics of LCs. First, a 5 μm spacer was applied to two AlTiSrO/rGO films. Afterwards, positive LC (IAN-5000XX T14, $\Delta n = 0.111$, $n_e = 1.595$, $n_o = 1.484$; JNC CO., Ltd.) was injected. Afterwards, the LC cell was manufactured through sealing through bonding at the edges. X-ray photoelectron spectroscopy (XPS,

K-alpha, Thermo VG, UK) was used to analyze the surface chemical composition and properties of the manufactured thin film. In addition, UV-Vis Spectrophotometers (V-650, JASCO Corp.) was used to measure the light transmittances of the thin films. The capacitance and voltage characteristics as well as EO properties (LCD evaluation system, LCMS-200, sesimlcd) of the thin films were analyzed through polarity fixed energy and residual DC voltage measurements (LCR Meter, 4284A, HP Agilent). Finally, the degree of LC alignment was measured via polarized optical microscopy (POM, BXP 51, Olympus) method.

3. RESULTS AND DISCUSSION

To determine the suitability of the AlTiSrO/rGO thin film for display devices according to annealing temperature, the results of measuring voltage-transmittance (VT) and

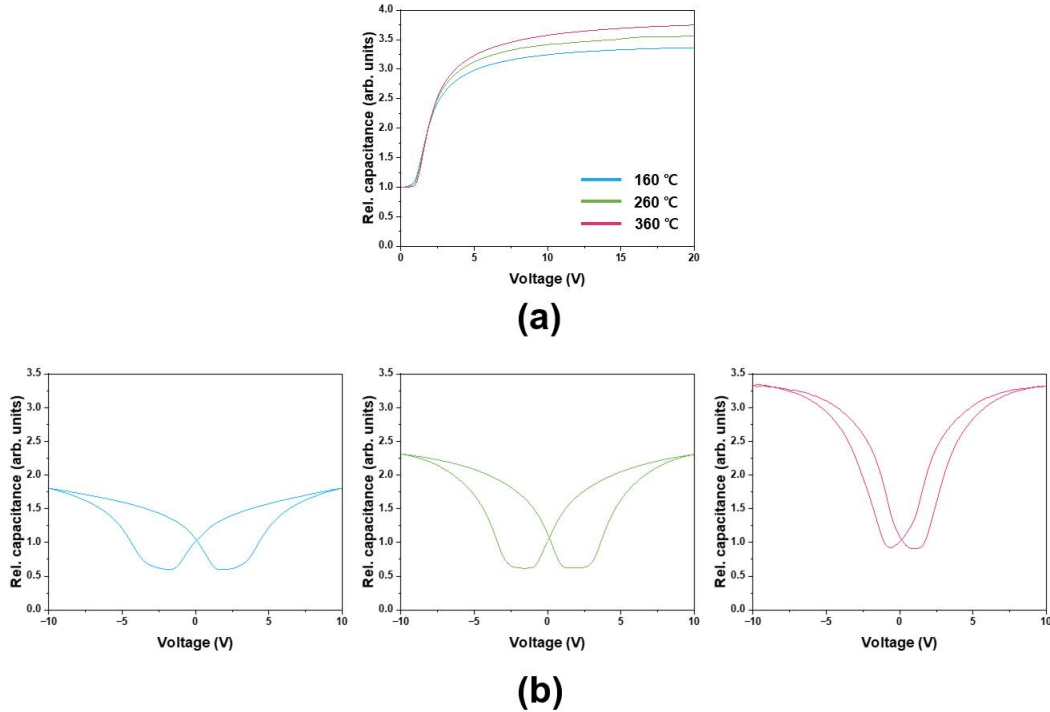


Fig. 3. Polar anchoring energy and residual dc graph for 160, 260, and 360°C
 그림 3. 160, 260, 및 360°C에 대한 극성 앵커링 에너지 및 잔류 dc 그래프

response time versus transmittance (RT) curves are shown in Fig. 2. Through the VT measurement in Fig. 2(a), the T90 values of AlTiSrO/rGO thin films at 160, 260, and 360°C decreased to 1.669 V, 1.518 V, and 1.598 V, respectively. Additionally, each transmittance values of the saturated region were 61%, 73%, and 83%, respectively. Additionally, the on-off values of AlTiSrO/rGO at 160, 260, and 360°C were 53.5-8.0, 22.7-11.3, and 26.2-25.5 ms, respectively. There was a clear decrease in response time due to the incorporation of annealing temperature. The shorter the response time, the better the clarity and smoothness of the screen by minimizing motion blur. Moreover, visual performance has

been improved through reduction of afterimage and latch effect, which are important disadvantages of the display. This highlights the transmittance characteristics of the display according to the application of the threshold voltage, and when annealing at 260°C, the highest transmittance efficiency was shown at the lowest voltage. As a result, it was confirmed that the response time increased significantly at a annealing of 260°C and the transmittance increased depending on the threshold voltage. This is a thin film suitable for low power consumption in display devices.

Surface anchoring energy is the energy required to displace a portion of the free energy within the thin film, reflecting the

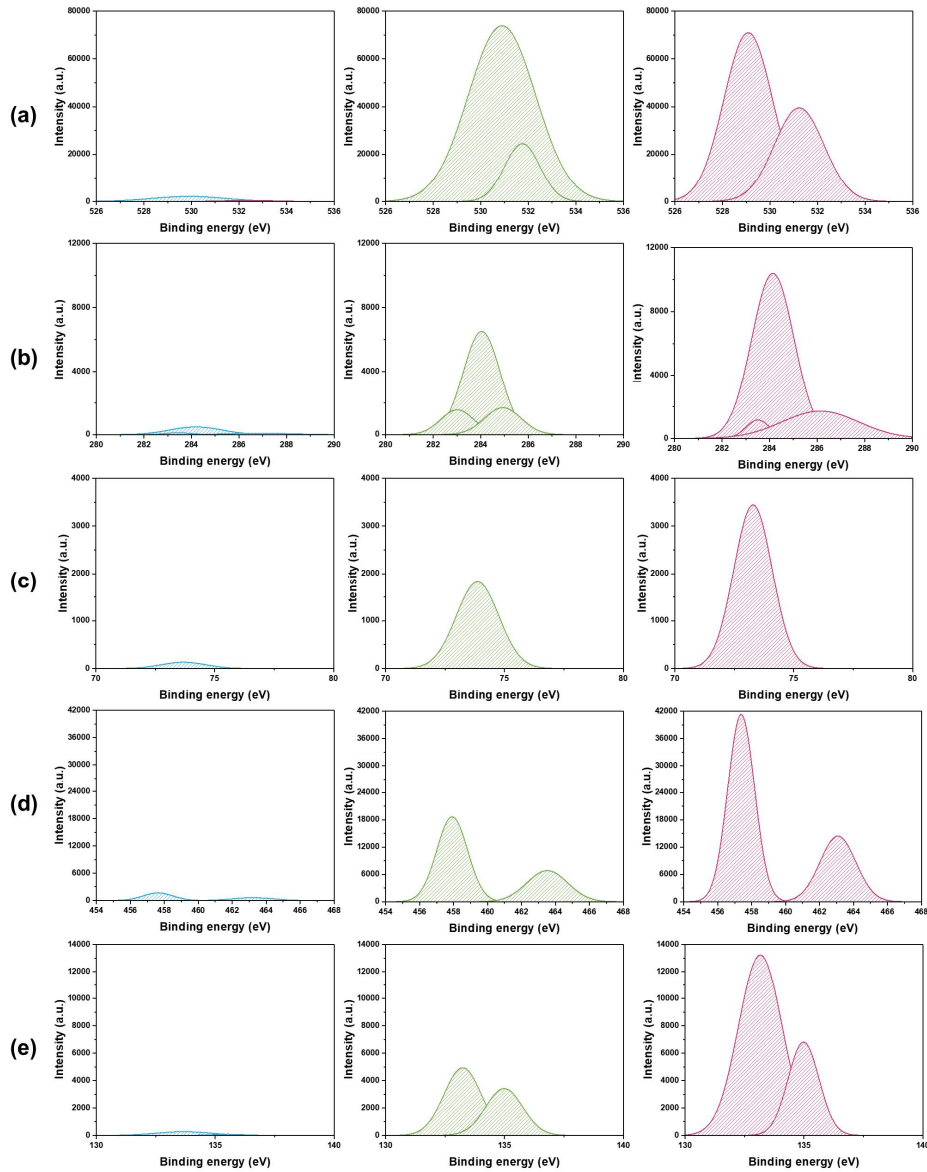


Fig. 4. High-resolution X-ray photoelectron spectroscopy was used to separate (a) O, (b) C, (c) Al, (d) Ti, and (e) Sr spectra of the hybrid films for 160, 260, and 360°C rGO to investigate intensity changes.

그림 4. 고해상도 X-선 광전자 분광법을 사용하여 160, 260 및 360°C에 대한 하이브리드 필름의 (a) O, (b) C, (c) Al, (d) Ti, 및 (e) Sr 스펙트럼 분리

strength of interaction between the liquid crystal molecules on the display cell surface and the alignment film. Fig. 3(a) shows that the

associated capacitance increases to 3.363, 3.566, and 3.747 at 160, 260, and 360°C. The obtained polar pinning energies are $1.28^{-4} \text{ Jm}^{-2}$,

$2.72^{-4} \text{ Jm}^{-2}$, and $6.66^{-3} \text{ Jm}^{-2}$, respectively. This increase in energy increases the available energy for free electrons to move as the annealing temperature increases, contributing to uniform alignment of liquid crystals between thin films. Hysteresis analysis was also performed with residual dc measurements and is shown in Fig. 3(b). Very wide hysteresis widths were observed at 160 and 260°C. However, at 360°C, the hysteresis width became very narrow, showing improved characteristics. Reducing the hysteresis width reduces the image fixation effect, which is a fatal drawback of LCD. Additionally, increasing the polarity anchoring energy can align the LC molecules more appropriately, resulting in better contrast ratio. Finally, less voltage is required to drive the LC molecules into the desired alignment, thus reducing power consumption.

rGO is composed of sp^2 and sp^3 carbon, and XPS measurements were performed to analyze changes in the carbon and oxygen functional groups during rGO doping, as shown in Figure 4. The primary binding energy peak for each element remained constant, and no binding energy shift occurred. Binding energy represents the energy required to remove an electron from an atom of a substance. First, Fig. 4(a) shows the O1s analysis. The binding energy peak of O1s is 531.38 eV. The intensities at 160, 260, and 360°C are 2810, 92644.4, and 80284.1, respectively. The peak table measurement results showed 51.51, 70.95, and 64.01%, respectively. Next, the peak of the carbon atom is shown in Fig. 4(b). The binding energy of C1s was 283.68 eV, and the intensities at 160, 260, and 360°C showed a gradually increasing trend to 975.2, 9623.8, and 22275.8. Fig. 4(c) showed the peak

analysis of Al2p element. It was found at a binding energy of 73.65 eV, and similarly, the intensity increased as the annealing temperature increased. This increase in intensity shows that the bonding of elements becomes stronger due to annealing. The peaks of Ti2p and Sr3d shown in (d) and (e) appeared at 457.9 eV and 133.23 eV, respectively, and the intensity increased as the annealing temperature increased. showed an increasing trend. This increase in inorganic material intensity is due to the rearrangement of elements, which increases the concentration of inorganic material elements in areas close to the surface. Additionally, as a reduction reaction occurs, the bond energy between elements changes and the intensity of the peak increases.

On the other hand, unlike the increase/decrease status of intensity as a result of XPS analysis, the element amount ratio in the peak table is shown in Table 1.

Table 1. Ratio of each element through peak table for XPS measurement results at 160, 260, and 360°C
표 1. 160, 260, 및 360°C에서 XPS 측정 결과에 대한 피크 표를 통한 각 원소의 비율

	160°C	260°C	360°C
O1s (%)	51.51	70.95	64.01
C1s (%)	26.00	18.01	13.99
Al2p (%)	7.37	3.62	6.21
Ti2p (%)	13.55	6.28	12.89
Sr3d (%)	1.57	1.15	2.9

As a result of the analysis, the proportion of oxygen elements was highest at 260°C. On the other hand, the ratio of inorganic elements (Al2p, Ti2p and Sr3d) was the lowest. Considering that the boiling point of 2-ME is 124°C, it can be seen that the solvent is completely removed at 260°C. When annealed at 360°C, oxygen vacancies increase due to more oxidation and reduction processes, but the total amount decreases. The

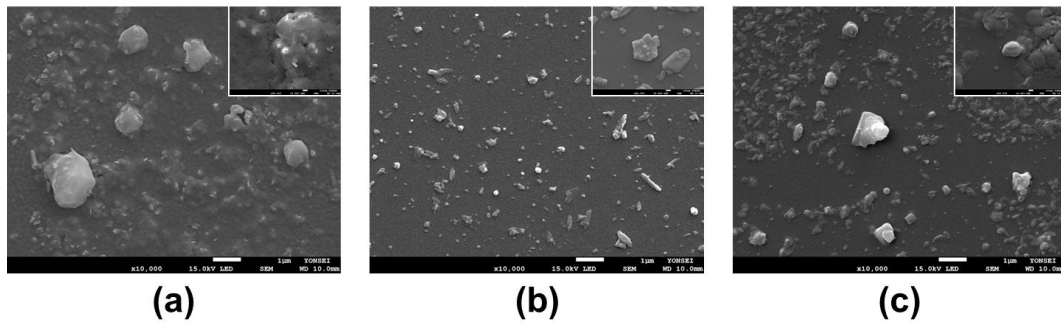


Fig. 5. Scanning electron microscopy measurements of (a) 160, (b) 260, and (c) 360°C AlTiSrO/rGO thin films
 그림 5. (a) 160, (b) 260, 및 (c) 360°C AlTiSrO/rGO 박막의 주사 전자 현미경 측정

proportion of carbon element decreases as the calcination temperature increases.

To analyze the surface atoms of AlTiSrO/rGO thin films according to annealing temperature, FE-SEM (IT-500HR, JEOL) was used, as shown in Figure 5. At 160, 260 and 360°C the amorphous surface image is clearly visible. The crystal size on the surface can be seen more clearly and larger at 360°C than at 260°C.

Figure 6 shows the results of POM analysis of the orientation state of LC molecules[22]. LC cells are analyzed using light microscopy between crossed polarizers.

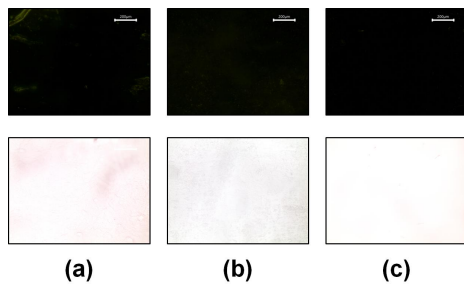


Fig. 6. Polarization microscopy analysis results images of AlTiSrO/rGO LC cell at different annealing temperatures: (a) 160°C, (b) 260°C, and (c) 360°C

그림 6. AlTiSrO/rGO LC 셀의 어닐링 온도 (a) 160°C, (b) 260°C, 및 (c) 360°C에 따른 각각의 편광현미경 분석결과 이미지

The black image means that the LC molecules are well aligned in the same direction as the surface. As a result, light is not scattered, resulting in a black image. On the other hand, when light scattering occurs between crossed polarizers and liquid crystal molecules, light leakage occurs, which means that the liquid crystal molecules are not well aligned. The optical refractive index anisotropy of the LC molecule causes scattering of downwardly polarized light. When an LC cell showing a well-aligned black image is rotated 45° between crossed polarizers, the bottom scattered light is uniformly aligned by the LC molecules and appears as bright light. This is called the white image of POM. Figure 6 (a), (b), and (c) show the POM results for AlTiSrO/rGO thin film at 160, 260, and 360°C, respectively. In the case of the dark image (a), light leakage clearly occurred. However, in (b) and (c), perfectly dark images were observed. In the white image, a blurry image is observed in (a) and (b), but a perfect white image is observed in (c). In other words, it can be seen that the liquid crystal molecules are completely aligned at 360°C. According to the results in Figure 3, which shows that the surface energy of the thin film

increases and becomes stable as the annealing temperature increases, the increase in surface energy and improved stability help the stable orientation of the liquid crystal as an alignment film.

Finally, to evaluate usability and suitability for display devices, the transmittance of the AlTiSrO/rGO thin film was measured at 160, 260 and 360°C, and the graph is shown in Figure 7. Transmittance was evaluated over the visible light wavelength range of 360-780 nm.

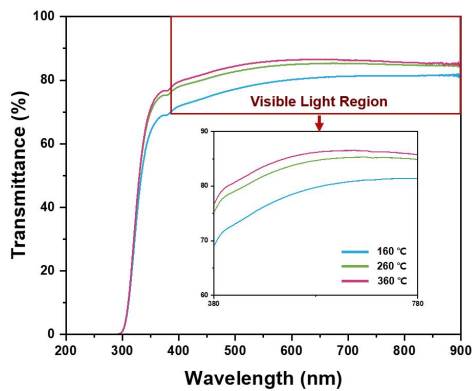


Fig. 7. Optical transmittances in the visible region for brush-coated AlTiSrO/rGO thin films at 160, 260, and 360°C
 그림 7. 160, 260, 및 360°C에서 브러시 코팅된 AlTiSrO/rGO 박막에 대한 가시영역의 광 투과율

The transmittance values for 160, 260 and 360°C were 82.00, 85.32, and 86.54%, respectively. Excellent results were obtained even though rGO is a black liquid. Additionally, considering that the commonly used PI rubbing film has a transmittance of about 80%, it was concluded that all AlTiSrO/rGO films are excellent for application to displays and photovoltaic devices.

4. CONCLUSION

In this study, a hybrid thin film was manufactured by doping graphene oxide into a sol-gel solution mixed with aluminum, titanium, and strontium oxide. The resulting hybrid AlTiSrO/rGO thin film features a microgroove anisotropic structure with amorphous properties because the groove structure was formed by brush coating. First, RT measurement analysis showed that the on-off value was significantly improved, stabilizing from 53.5-8.0 ms at 160°C to 26.2-25.5 ms at 360°C annealing. Additionally, through VT measurement analysis, the T90 value decreased from 1.669V to 1.598V. Additionally, XPS analysis revealed changes in the chemical composition of the thin film surface due to rGO doping. The incorporation of rGO strengthened the inorganic material through covalent bonding of sp^3 hybrid carbon atoms, resulting in the removal or reduction of oxygen functional groups and reduction of oxygen vacancies. It was shown that these oxygen vacancies increased as the annealing temperature increased. Additionally, SEM analysis clearly showed rGO on the AlTiSrO/rGO surface. Finally, as a result of transmittance measurement, the AlTiSrO/rGO thin film annealed at 360°C showed a transmittance of 86.54%, which is very excellent compared to commercially available rubbing PI films. As a result, these thin films have potential applications in display, semiconductor, and solar energy fields due to their outstanding properties, making them a potential next-generation thin film.

REFERENCES

- [1] D. V. D. O. Henriquez, M. Kang, I. Cho, J. Choi, J. Park, O. Gul, J. Ahn, D.-S. Lee, and I. Park, "Low-Power, Multi-Transduction Nanosensor Array for Accurate Sensing of Flammable and Toxic Gases" *Small methods*, vol. 7, no. 3, pp. 2201352, 2023.
- [2] W. Hou, J. Li, Z. Cao, S. Lin, C. Pan, Y. Pang, and J. Liu, "Decorating Bacteria with a Therapeutic Nanocoating for Synergistically Enhanced Biotherapy", *Small*, vol. 17, no. 37, pp. 2101810, 2021.
- [3] S. Blankenburg, M. Bieri, R. Fasel, K. Müllen, C. A. Pignedoli, and D. Passerone, "Porous Graphene as an Atmospheric Nanofilter", *Small*, vol. 6, no. 20, pp. 262-2271, 2010.
- [4] Y. Sasaki and K. Akiyoshi, "Nanogel engineering for new nanobiomaterials: from chaperoning engineering to biomedical applications", *The Chemical Record*, vol. 10, no. 6, pp. 366-376, 2010.
- [5] D. Yoo, S. Kim, W. Cho, J. Park, and J. Kim, "Hydroprinting Technology to Transfer Ultrathin, Transparent, and Double-Sided Conductive Nanomembranes for Multiscale 3D Conformal Electronics", *Small methods*, vol. 6, no. 1, pp. 2100869, 2022.
- [6] Y. J. Kim, Z. Zhuang, and J. S. Patel, "Effect of multidirection rubbing on the alignment of nematic liquid crystal ", *Applied Physics Letters*, vol. 77, no. 4, pp. 513-515, 2000.
- [7] S. Varghese, S. Narayanankutty, C. W. M. Bastiaansen, G. P. Crawford, and D. J. Broer, "Patterned Alignment of Liquid Crystals by μ -Rubbing", *Advanced Materials*, vol. 16, no. 18, pp. 1600-1605, 2004.
- [8] J.-H. Kim, M. Yoneya, and H. Yokoyama, "Tristable nematic liquid-crystal device using micropatterned surface alignment", *Nature*, vol. 420, no. 6912, pp. 159-162, 2002.
- [9] I. H. Song, H.-C. Jeong, J. H. Lee, J. Won, D. H. Kim, D. Lee, J. Y. Oh, J. I. Jang, Y. Liu, and D.-S. Seo, "Selective Liquid Crystal Driving Mode Achieved by Controlling the Pretilt Angle via a Nanopatterned Organic/Inorganic Hybrid Thin Film", *Advanced Optical Materials*, vol. 9, no. 9, pp. 2001639, 2021.
- [10] T.-T.-T. Nguyen, T.-N. Luu, D.-H. Nguyen, and T.-T. Duong, "Comparative Study on Backlighting Unit Using CsPbBr₃ Nanocrystals/KSFM Phosphor + Blue LED and Commercial WLED in Liquid Crystal Display", *Journal of Electronic Materials*, vol. 50, pp. 1827-1834, 2021.
- [11] W.-K. Lee, Y. S. Choi, Y.-G. Kang, J. Sung, D.-S. Seo, and C. Park, "Super-Fast Switching of Twisted Nematic Liquid Crystals on 2D Single Wall Carbon Nanotube Networks", *Advanced Functional Materials*, vol. 21, no. 20, pp. 3843-3850, 2011.
- [12] H. Hosono, H. Ohta, M. Orita, K. Ueda, and M. Hirano, "Frontier of transparent conductive oxide thin films", *Vacuum*, vol. 66, no. 3-4, pp. 419-425, 2002.
- [13] M. G. Mason, L. S. Hung, C. W. Tang, S. T. Lee, K. W. Wong, and M. Wang, "Characterization of treated indium-tin-oxide surfaces used in electroluminescent devices", *Journal of Applied Physics*, vol. 86, no. 3, pp. 1688-1692, 1999.
- [14] C. A. Mirkin and W. B. Caldwell, "Thin film, Fullerene-Based Materials" *Tetrahedron*, vol. 52, no. 14, pp. 5113-5130, 1996.
- [15] L. Hu, D. S. Hecht, and G. Grüner, "Carbon Nanotube Thin Films: Fabrication, Properties, and Applications", *Chemical Reviews*, vol. 110, no. 10, pp. 5790-5844, 2010.
- [16] Y. Liu, H. Zhou, N. O Weiss, Y. Huang, and X. Duan, "High-Performance Organic Vertical Thin Film Transistor Using Graphene as a Tunable Contact", *ACS Nano*, vol. 9, no. 11, pp. 11102-11108, 2015.
- [17] İ. Karteri, Ş. Karataş, A. A. Al-Ghamdi, and F. Yakuphanoglu, "The Electrical Characteristics of Thin Film Transistors with Graphene Oxide and Organic Insulators", *Synthetic Metals*, vol. 199, pp. 241-245, 2015.
- [18] Y. H. Shim, K. E. Lee, T. J. Shin, S. O. Kim, and S. Y. Kim, "Tailored Colloidal Stability and Rheological Properties of Graphene Oxide Liquid Crystals with Polymer-Induced Depletion Attractions", *ACS Nano*, vol. 12, no.

- 11, pp. 11399-11406, 2018.
- [19] S.-H. Hong, T.-Z. Shen, and J.-K. Song, "Electro-Optical Characteristics of Aqueous Graphene Oxide Dispersion Depending on Ion Concentration", *The Journal of Physical Chemistry C*, vol. 118, no. 45, pp. 26304-26312, 2014.
- [20] T.-Z. Shen, S.-H. Hong, and J.-K. Song, "Electro-Optical Switching of Graphene Oxide Liquid Crystals with an Extremely Large Kerr Coefficient", *Nature Materials*, vol. 13, no. 4, pp. 394-399, 2014.
- [21] J.-i. Fukuda, M. Yoneya, and H. Yokoyama, "Surface-Groove-Induced Azimuthal Anchoring of a Nematic Liquid Crystal: Berreman's Model Reexamined", *Physical Review Letters*, vol. 98, no. 18, pp. 187803, 2007.
- [22] D. W. Berreman, "Solid Surface Shape and the Alignment of an Adjacent Nematic Liquid Crystal", *Physical Review Letters*, vol. 28, no. 26, pp. 1683-1686, 1972.

Author Biography

오 병 윤 (Byeong-Yun Oh) [Regular Member]



- 2004. 02: Physics, Hanseo University (B.S.)
- 2006. 02: Metallurgical Engineering, Yonsei University (M.S.)
- 2011. 02: Electrical and Electronic Engineering, Yonsei University (Ph.D.)
- 2015. 01 ~ 2018. 04: CEO, ZeSHTech Co., Ltd.
- 2020. 06 ~ Present: Senior Managing Director, CheomdanLab Inc.

⟨Interests⟩ Liquid crystal alignment layer, thin film transistor device, dye-sensitized solar cell module